Preparation, Structure, and Reactions of a Lattice-Framework Disilene

Shinobu Tsutsui,*,† Eunsang Kwon,† Hiromasa Tanaka,† Shigeki Matsumoto,† and Kenkichi Sakamoto*,†,‡

Photodynamics Research Center, The Institute of Physical and Chemical Research (RIKEN), 519-1399 Aoba, Aramaki, Aoba-ku, Sendai 980-0845, Japan, and Department of Chemistry, Graduate School of Science, Tohoku University, Aoba-ku, Sendai 980-8578, Japan

Received May 9, 2005

Reduction of tri-*tert*-butyl-3-(tribromosilyl)cyclopropene with potassium graphite yielded a unique lattice-framework disilene, a racemate of (4*R*,6*R*,4′*R*,6′*R*)- and (4*S*,6*S*,4′*S*,6′*S*)-2,3,4,6,7,8,2′,3′,4′,6′,7′,8′-dodeca-*tert*-butyl-[5,5′]bi{1,5-disilatricyclo[4.2.0.0^{1,4}]octylidene}-2,7,2′,7′-tetraene (*dl*-**2**). Oxidation of *dl*-**2** gave the corresponding 1,3,2,4-dioxadisiletane derivative stereospecifically. Trapping experiments revealed that a thermal equilibrium between *dl*-**2** and the corresponding silylene, 2,3,4,6,7,8-hexa-*tert*-butyl-1,5-disilatricyclo-[4.2.0.0^{1,4}]octa-2,7-diene-5,5-diyl (**6**), existed in solution at room temperature. Thus, the intermediate **6** reacted with methanol, halides, and acetylenes to give the corresponding methoxysilane, dihalosilanes, and silacyclopropenes, respectively. The reactions were accelerated by irradiation. DFT calculations of *dl*-**2** and the related compounds well reproduced the experimental results of the thermal equilibrium between *dl*-**2** and **6**. TD-DFT calculations of *dl*-**2** revealed that an intramolecular through-space interaction exists between the $\pi^*_{Si=Si}$ and $\pi^*_{C=C}$ orbitals in the LUMO of *dl*-**2**, contributing to the stabilization of the LUMO.

Introduction

Silicon−silicon multiple-bonded compounds have been comprehensively studied since the first isolation of Mes_2-Si=$SiMes_2$ (Mes = 2,4,6-trimethylphenyl) by West et al. in 1981.[1] At present, not only various types of acyclic and cyclic disilenes[2] (silicon−silicon double-bonded compounds) but also a trisilaallene[3] and disilynes[4] (silicon−silicon triple-bonded compounds) are known to be stable compounds. Most stable silicon−silicon multiple-bonded compounds are stabilized by inert bulky substituents. It is noteworthy that a *Z*-1,2-diamino-1,2-disilyldisilene derivative is prepared by tetramerization of a cyclic diaminosilylene.[5]

Dissociation of the disilene into the corresponding silylene is rare because of the thermal stability of the disilene.[2] Okazaki et al. reported the reversible dissociation of a crowded tetraaryldisilene, Tbt(Mes)Si=Si(Mes)Tbt, into Tbt(Mes)Si: (Tbt = 2,4,6-tris[bis-(trimethylsilyl)methyl]phenyl).[6,7] The thermal equilibrium between amino-substituted disilenes and the corresponding silylenes has also been reported.[5,8] While the photochemical dissociation of Dis_2Si=$SiDis_2$ (Dis = bis-(trimethylsilyl)methyl) into the corresponding silylene was reported,[9a] the thermal dissociation of a tetraalkyldisilene has not been reported. Although tetraalkyldisilenes such as tetramethyldisilene have been widely investigated from the viewpoints of the spectroscopic and theoretical interests, X-ray crystallographic analysis of tetraalkyldisilenes has not been reported yet.

On the other hand, cyclopropene is one of the smallest ring compounds and has a highly strained energy.[10] Therefore, cyclopropenes having a reactive site easily give a variety of isomerized and ring-opened com-

* Corresponding authors. E-mail: stsutsui@riken.jp; sakamoto@si.chem.tohoku.ac.jp.
† RIKEN.
‡ Tohoku University.

(1) West, R.; Fink, M. J.; Michl, J. *Science* **1981**, *214*, 1343.
(2) For recent reviews on disilenes, see: (a) Iwamoto, T.; Kira, M. *J. Synth. Org. Chem.* **2004**, *62*, 94. (b) Sekiguchi, A.; Lee, V. Ya. *Chem. Rev.* **2003**, *103*, 1429. (c) Weidenbruch, M. *J. Organomet. Chem.* **2002**, *646*, 39. (d) Weidenbruch, M. In *The Chemistry of Organic Silicon Compounds III*; Rappoport Z.; Apeloig, Y., Eds.; Wiley: Chichester, 2001; p 391. (e) West, R. *Polyhedron* **2002**, *21*, 467. (f) Kira, M.; Iwamoto, T. *J. Organomet. Chem.* **2000**, *611*, 236. (g) Tokitoh, N.; Okazaki, R. *Coord. Chem. Rev.* **2000**, *210*, 251. (h) Gaspar, P. P.; West, R. In *The Chemistry of Organic Silicon Compounds*, 2nd ed.; Rappoport, Z., Apeloig, Y., Eds.; John Wiley & Sons: New York, 1999; Part 3, p 2463. (i) Okazaki, R.; West, R. *Adv. Organomet. Chem.* **1996**, *39*, 231. (j) Weidenbruch, M. *Coord. Chem. Rev.* **1994**, *130*, 275. (k) Grev, R. S. *Adv. Organomet. Chem.* **1991**, *33*, 125. (l) Tsumuraya, T.; Batcheller, S. A.; Masamune, S. *Angew. Chem., Int. Ed. Engl.* **1991**, *30*, 902. (m) Raabe, G.; Michl, J. In *The Chemistry of Organic Silicon Compounds, Part 2*; Patai S., Rappoport, Z., Eds.; Wiley: New York, 1989; Chapter 17. (n) West, R. *Angew. Chem., Int. Ed. Engl.* **1987**, *26*, 1201. (o) Raabe, G.; Michl, *J. Chem. Rev.* **1985**, *85*, 5. (p) West, R. *Pure Appl. Chem.* **1984**, *56*, 163.
(3) Ishida, S.; Iwamoto, T.; Kabuto C.; Kira, M. *Nature* **2003**, *421*, 725.
(4) (a) Sekiguchi, A.; Kinjo, R.; Ichinohe, M. *Science* **2004**, *305*, 1755. (b) Wiberg, N.; Vasisht, S. K.; Fischer, G.; Mayer, P. *Z. Anorg. Allg. Chem.* **2004**, *630*, 1823.
(5) Schmedake, T. A.; Haaf, M.; Apeloig, Y.; Müller, T.; Bukalov, S.; West, R. *J. Am. Chem. Soc.* **1999**, *121*, 9479.
(6) Tokitoh, N.; Suzuki, H.; Okazaki, R.; Ogawa, K. *J. Am. Chem. Soc.* **1993**, *115*, 10428.
(7) Suzuki, H.; Tokitoh, N.; Okazaki, R. *Bull. Chem. Soc. Jpn.* **1995**, *68*, 2471.
(8) Tsutsui, S.; Sakamoto, K.; Kira, M. *J. Am. Chem. Soc.* **1998**, *120*, 9955.
(9) (a) Masamune, S.; Eriyama, Y.; Kawase, T. *Angew. Chem., Int. Ed. Engl.* **1987**, *26*, 584. (b) West, R.; Cavalieri, J. D.; Buffy, J. J.; Fry, C.; Zilm, K. W.; Duchamp, J. C.; Kira, M.; Iwamoto, T.; Müller, T.; Apeloig, Y. *J. Am. Chem. Soc.* **1997**, *119*, 4972.

10.1021/om050362l CCC: $30.25
Publication on Web 08/11/2005

Scheme 1

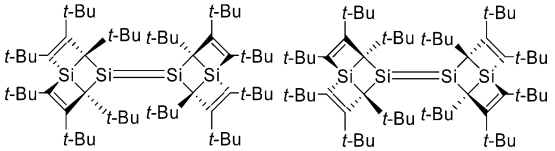

(4*R*,6*R*,4′*R*,6′*R*)-**2** + (4*S*,6*S*,4′*S*,6′*S*)-**2** = *dl*-**2**

pounds.[10−13] For more than a decade, we have investigated the chemistry of silicon-substituted cyclopropenes, such as hexasilylbicyclopropenyls[14] and 4-silatriafulvenes.[15] In the course of our study, we found the unexpected reactivity of a trihalosilyl-substituted cyclopropene.

In a preliminary contribution, we reported that reduction of tri-*tert*-butyl-3-(tribromosilyl)cyclopropene (**1a**) with potassium graphite gave a unique lattice-framework disilene, a racemate of (4*R*,6*R*,4′*R*,6′*R*)- and (4*S*,6*S*,4′*S*,6′*S*)-2,3,4,6,7,8,2′,3′,4′,6′,7′,8′-dodeca-*tert*-butyl-[5,5′]bi{1,5-disilatricyclo[4.2.0.0^{1,4}]octylidene}-2,7,2′,7′-tetraene (*dl*-**2**), as shown in Scheme 1.[16] Also, a few characteristic reactivities and properties of *dl*-**2** were described in our communications.[17,18] In this paper, we describe the details of the preparation, structure, and reactions of *dl*-**2**.

Results and Discussion

Preparation of Disilene *dl*-2. A precursor, tri-*tert*-butyl-3-(tribromosilyl)cyclopropene (**1a**), for the synthesis of disilene *dl*-**2** was prepared according to the method shown in Scheme 2. The reaction of tri-*tert*-butylcyclopropenyium tetrafluoroborate[19] with triphenylsilyllithium in THF gave tri-*tert*-butyl-3-(triphenylsilyl)cyclopropene (**3**) in 90% yield. Bromodephenylation of **3** with

Scheme 2

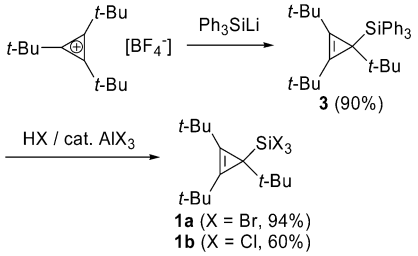

Scheme 3

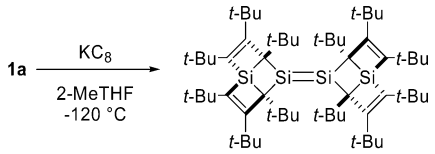

dl-**2** (55%)

dry hydrogen bromide in the presence of a catalytic amount of aluminum bromide provided **1a** in 94% yield. Similarly, tri-*tert*-butyl-3-(trichlorosilyl)cyclopropene (**1b**) was prepared by chlorodephenylation of **3** in 60% yield.

Reductive dehalogenation of **1a** by potassium graphite (KC_8) in 2-methyltetrahydrofuran (2-MeTHF) at −120 °C for 24 h gave *dl*-**2** as red-orange crystals in 55% yield (Scheme 3). Disilene *dl*-**2** was isolated by recrystallization from hexane. The low reaction temperature was very effective for the productivity of *dl*-**2**, because the similar reduction of **1a** in THF at −80 °C for 24 h gave *dl*-**2** in only 16% yield. In contrast with **1a**, reduction of **1b** with KC_8 under similar conditions gave the reaction mixture including a trace amount of *dl*-**2**. The structure of *dl*-**2** was established using mass spectrometry and ^{1}H, ^{13}C, and ^{29}Si NMR spectroscopy and confirmed by X-ray crystallographic analysis. Disilene *dl*-**2** was stable up to 257 °C in the solid state under oxygen-free conditions, and no change was observed on heating of a C_7D_8 solution of *dl*-**2** under oxygen-free condition in a sealed NMR tube at 70 °C for 14 h.

X-ray Crystallographic Analysis of *dl*-2. A single crystal of *dl*-**2**, suitable for X-ray crystallographic analysis, was obtained by recrystallization from toluene. X-ray crystallographic analysis of *dl*-**2** confirmed that *dl*-**2** is a racemate of (4*R*,6*R*,4′*R*,6′*R*)-**2** and (4*S*,6*S*,4′*S*,6′*S*)-**2** (Scheme 1). The observed molecular structure of *dl*-**2** is shown in Figure 1. Selected bond lengths and angles for *dl*-**2** are shown in Figure 2. Crystal data and structure refinement for *dl*-**2** are summarized in Table 1. Disilene *dl*-**2** has C_2 symmetry through the axis perpendicular to the plane involving two Si_2C_2 rings, and *dl*-**2** has six kinds of crystallographically nonequivalent *tert*-butyl groups in the solid state. The silicon−silicon double-bond length of *dl*-**2** is 2.2621(15) Å, which is the longest of all carbon-substituted disilenes reported.[2] The bent angle defined by Si1*=Si1- -Si2 is 177.75(3)°. The unsaturated silicon atom Si1 is not pyramidized, and the sum of the bond angles around the Si1 is 360°. The central 1,3-disilacyclobutane rings (Si1−C1−Si2−C6) are almost planar (within 0.018 Å

(10) For recent reviews on cyclopropenes, see: (a) Komatsu, K.; Kitagawa, T. *Chem. Rev.* **2003**, *103*, 1371. (b) Billups, W. In *The Chemistry of the Cyclopropyl Group*; Patai, S., Rappoport, A., Eds.; Wiley Interscience: New York, 1987. (c) Komatsu, K.; Yoshida, Z. In *Methods of Organic Chemistry (Houben-Weyl)*; de Meijere, A., Ed.; Thieme: Stuttgart, 1996; Vol. E17d, pp 3079−3192.

(11) (a) Maier, G.; Neudert, J.; Wolf, O.; Pappusch, D.; Sekiguchi, A.; Tanaka, M.; Matsuo, T. *J. Am. Chem. Soc.* **2002**, *124*, 13819. (b) Maier, G.; Kratt, A.; Schick, A.; Reisenauer, H. P.; Barbosa, F.; Gescheidt, G. *Eur. J. Org. Chem.* **2000**, 1107. (c) Maier, G.; Born, D.; Bauer, I.; Wolf, R.; Boese, R.; Cremer, D. *Chem. Ber.* **1994**, *127*, 173.

(12) (a) Fink, M. J.; Puranik, D. B. *Organometallics* **1987**, *6*, 1809. (b) Fink, M. J., Puranik, D. B.; Johnson, M. P. *J. Am. Chem. Soc.* **1988**, *110*, 1315. (c) Puranik, D. B.; Fink, M. J. *J. Am. Chem. Soc.* **1989**, *111*, 5951. (d) Puranik, D. B.; Johnson, M. P.; Fink, M. J. *Organometallics* **1989**, *8*, 770. (e) Gee, J. R.; Howard, W. A.; McPherson, G. L.; Fink, M. J. *J. Am. Chem. Soc.* **1991**, *113*, 5461.

(13) Schick, A. Doctral Dissertation, Universität Giessen, Germany, 1992.

(14) Sakamoto, K.; Saeki, T.; Sakurai, H. *Chem. Lett.* **1993**, 1675.

(15) (a) Sakamoto, K.; Ogasawara, J.; Sakurai, H.; Kira, M. *J. Am. Chem. Soc.* **1997**, *119*, 3405. (b) Veszpremi, T.; Takahashi, M.; Ogasawara, J.; Sakamoto, K.; Kira, M. *J. Am. Chem. Soc.* **1998**, *120*, 2408. (c) Veszpremi, T.; Takahashi, M.; Hajgato, B.; Ogasawara, J.; Sakamoto, K.; Kira, M. *J. Phys. Chem. (A)* **1998**, *102*, 10530. (d) Takahashi, M.; Sakamoto, K.; Kira, M. *Int. J. Quantum Chem.* **2001**, *84*, 198. (e) Sakamoto, K.; Ogasawara, J.; Kon, Y.; Sunagawa, T.; Kira, M. *Angew. Chem., Int. Ed.* **2002**, *41*, 1402. (f) Kon, Y.; Ogasawara, J.; Sakamoto, K.; Kabuto, C.; Kira, M. *J. Am. Chem. Soc.* **2003**, *125*, 9310. (g) Kon, Y.; Sakamoto, K.; Kabuto, C.; Kira, M. *Organometallics* **2005**, *24*, 1407.

(16) Matsumoto, S.; Tsutsui, S.; Kwon, E.; Sakamoto, K. *Angew. Chem., Int. Ed.* **2004**, *43*, 4610.

(17) Tsutsui, S.; Tanaka, H.; Kwon, E.; Matsumoto, S.; Sakamoto, K. *Organometallics* **2004**, *23*, 5659.

(18) Tanaka, H.; Kwon, E.; Tsutsui, S.; Matsumoto, S.; Sakamoto, K. *Eur. J. Inorg. Chem.* **2005**, 1235.

(19) (a) Ciabattoni, J.; Nathan, E. C.; Feiring, A. E.; Kocienski, P. J. *Org. Synth.* **1974**, *54*, 97. (b) Ciabattoni, J.; Nathan, E. C.; Feiring, A. E.; Kocienski, P. J. *Organic Syntheses*; Wiley: New York, 1988; Collect. Vol. 6, p 991.

Table 1. Crystal Data and Structure Refinement for *dl*-2, *dl*-4, and 7a

	dl-**2**	*dl*-**4**	**7a**
formula	$C_{60}H_{108}Si_4$	$C_{60}H_{108}O_2Si_4$	$C_{38}H_{72}Si_4$
fw	941.82	973.82	641.32
temp (K)	123(2)	123(2)	123(2)
cryst description	red-orange plate	colorless plate	colorless plate
cryst size (mm^3)	0.21 × 0.18 × 0.10	0.35 × 0.33 × 0.24	0.40 × 0.32 × 0.27
cryst syst	orthorhombic	orthorhombic	monoclinic
space group	*Pcca*	*Pbcn*	*C*2/*c*
a (Å)	28.034(5)	57.045(10)	21.118(5)
b (Å)	19.327(3)	10.814(2)	13.125(3)
c (Å)	10.7343(19)	28.405(5)	17.174(4)
α (deg)	90	90	90
β (deg)	90	90	121.528(3)
γ (deg)	90	90	90
V ($Å^3$)	5816.0(17)	17523(5)	4057.5(17)
Z	4	12	4
ρ_{calcd} (Mg/m^3)	1.076	1.107	1.050
abs coeff (mm^{-1})	0.137	0.141	0.170
F(000)	2096	6479	1424
θ range for data collection (deg)	1.45 to 25.99	2.28 to 26.66	1.92 to 26.00
index range	$-34 \le h \le 33$	$-69 \le h \le 70$	$-23 \le h \le 26$
	$-17 \le k \le 23$	$-11 \le k \le 13$	$-16 \le k \le 10$
	$-13 \le l \le 13$	$-21 \le l \le 21$	$-21 \le l \le 21$
no. of reflns collected	30 861	94 561	10 960
no. of ind reflns	5719	17 237	3971
R(int)	0.0876	0.1157	0.0607
no. of reflns with $I > 2\sigma(I)$	3684	10 999	3495
no. of data/restraints/params	5719/0/307	17 237/0/946	3971/0/203
goodness-of-fit on F^2	1.027	1.078	1.068
final R indices $[I > 2\sigma(I)]^a$	R1 = 0.0618	R1 = 0.0817	R1 = 0.0443
	wR2 = 0.1475	wR2 = 0.1837	wR2 = 0.1195
R indices (all data)	R1 = 0.1054	R1 = 0.1294	R1 = 0.0493
	wR2 = 0.1730	wR2 = 0.2040	wR2 = 0.1238
largest diff peak and hole (e $Å^{-3}$)	0.361 and −0.240	0.579 and −0.553	0.531 and −0.295

[a] $R1 = \sum||F_o| - |F_c||/\sum|F_o|$. $wR2 = [\sum[w(F_o^2 - F_c^2)^2]/\sum[w(F_o^2)^2]]^{0.5}$.

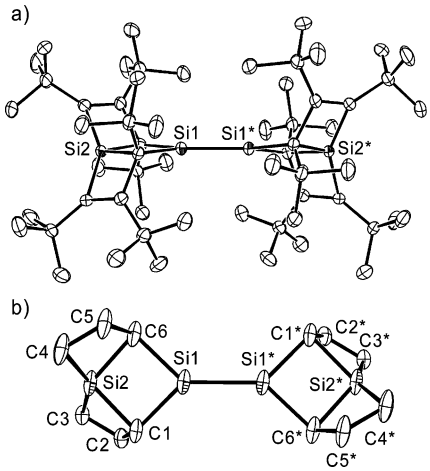

Figure 1. (a) Side and (b) top ORTEP views of *dl*-**2**. Thermal ellipsoids are drawn at the 50% probability level. Hydrogen atoms (a and b) and *tert*-butyl groups (b) are omitted for clarity.

from their least-squares plane), and the C1−Si1−Si1*−C6* dihedral angle is 12.1°. While carbon-substituted disilenes generally adopt trans-bent structures,[21] the structure of *dl*-**2** around the disilene moiety is not bent but slightly twisted. The torsion angles of Si1*−Si1−C1−C2 and Si1*−Si1−C6−C5 are 96.7° and 102.9°, respectively. The torsion angles of C1−C2−C3−Si2 (13.7°) and C6−C5−C4−Si2 (15.8°) indicate that the silacyclobutene rings are twisted. It is noteworthy that the C3−Si2−C4 bond angle is 147.40(12)°, which is apparently distorted from the ideal bond angle in an sp^3 silicon atom (109.5°).

Spectral Properties of *dl*-2. The ^1H NMR spectrum of *dl*-**2** in C_6D_6 showed three kinds of peaks assignable to the *tert*-butyl groups. The result suggests that *dl*-**2** has C_2 symmetry through the Si=Si bond in solution. A significant temperature dependence of the signals of *dl*-**2** was not observed in C_7D_8 between 20 and 110 °C. The ^{29}Si NMR spectrum of *dl*-**2** showed two peaks at −36.7 and 102.5 ppm. The former and the latter are assignable to the sp^3 silicon atom and the unsaturated silicon atom, respectively. The observed ^{29}Si chemical shift of the unsaturated silicon in *dl*-**2** is similar to those in $Dis_2Si{=}SiDis_2$ (90.4 ppm)[9b] and *trans*-Mes(*t*-Bu)Si=SiMes(*t*-Bu) (90.3 ppm).[22a]

The UV−vis absorption maximum of the $\pi-\pi^*$ transition band of *dl*-**2** in hexane at room temperature was observed at 493 nm. This value indicates that the transition band was red-shifted relative to the typical values for the tetraalkyldisilene: tetramethyldisilene (350 nm)[23] and $Dis_2Si{=}SiDis_2$ (393 nm).[9a] A significant temperature dependence of the absorption maximum of

(20) (a) Conlin, R. T.; Zhang, S.; Namavari, M.; Bobbitt, K. L.; Fink, M. J. *Organometallics* **1989**, *8*, 571. (b) Steinmetz, M. G.; Udayakumar, B. S.; Gordon, M. S. *Organometallics* **1989**, *8*, 530.

(21) (a) Krogh-Jespersen, K. *J. Phys. Chem.* **1982**, *86*, 1492. (b) Olbrich, G. *Chem. Phys. Lett.* **1986**, *130*, 115. (c) Somasundram, K.; Amos, R. D.; Handy, N. C. *Theor. Chim. Acta* **1986**, *70*, 393. (d) Teramae, H. *J. Am. Chem. Soc.* **1987**, *109*, 4140. (e) Sari, L.; McCarthy, M. C.; Schaefer, H. F.; Thaddeus, P. *J. Am. Chem. Soc.* **2003**, *125*, 11409.

(22) (a) Fink, M. J.; Michalczyk, M. J.; Haller, K. J.; West, R.; Michl, J. *Organometallics* **1984**, *3*, 793. (b) Iwamoto, T.; Masuda, H.; Ishida, S.; Kabuto, C.; Kira, M. *J. Am. Chem. Soc.* **2003**, *125*, 9300. (c) Suzuki, H,; Tokitoh, N.; Okazaki, R. Harada, J.; Ogawa, K.; Tomoda, S.; Goto, M. *Organometallics* **1995**, *14*, 1016.

(23) Sekiguchi, A.; Maruki, I.; Ebata, K.; Kabuto, C.; Sakurai, H. *J. Chem. Soc., Chem. Commun.* **1991**, 341.

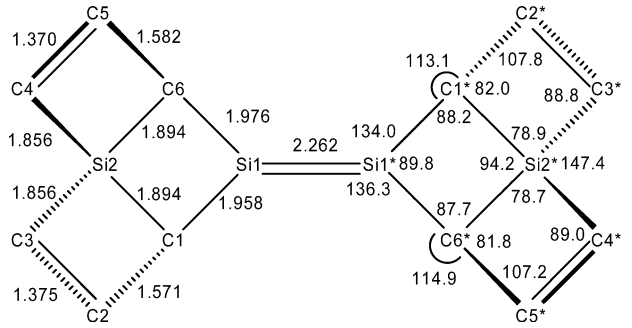

Figure 2. Selected bond lengths (Å) and angles (deg) for *dl*-**2**.

Scheme 4

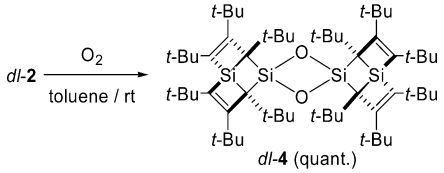

dl-**2** was not observed in 3-methylpentane (3-MP) or methylcyclohexane between −196 and 100 °C.

The resonance Raman spectrum of *dl*-**2** showed a broad line appearing at 548 cm^{-1} assignable to a symmetric Si=Si vibration. The value was similar to that for $Mes_2Si{=}SiMes_2$ (539 cm^{-1}), $Dis_2Si{=}SiDis_2$ (522 cm^{-1}), and *trans*-Mes(*t*-Bu)Si=SiMes(*t*-Bu) (525 cm^{-1}).[1,24]

Oxidation of *dl*-2. A toluene solution of *dl*-**2** under an oxygen atmosphere was stirred at room temperature for 1 week to yield the corresponding 1,3,2,4-dioxadisiletane derivative *dl*-**4** quantitatively, as shown in Scheme 4. The structure of *dl*-**4** was established using mass spectrometry and ^1H, ^{13}C, and ^{29}Si NMR spectroscopy and confirmed by X-ray crystallographic analysis.

X-ray crystallographic analysis of *dl*-**4** revealed that oxidation of *dl*-**2** proceeded stereospecifically.[7,22a] A single crystal of *dl*-**4**, suitable for X-ray crystallographic analysis, was obtained by recrytallization from toluene. Crystal data and structure refinement for *dl*-**4** are summarized in Table 1. The asymmetric units of *dl*-**4** contain two crystallographically independent molecules, molecules **4A** and **4B**. As shown in Figure 2 and Figure 3, molecule **4A** has C_1 symmetry and molecule **4B** has C_2 symmetry. The characteristic features of molecules **4A** and **4B** are fundamentally similar, as shown in Figure 4. The average Si- - -Si distance and Si−O bond lengths in the Si_2O_2 ring of *dl*-**4** are 2.466 and 1.697 Å, respectively. The values are similar to that of $R_2SiO_2SiR_2$ (R_2Si = 2,2,5,5-tetrakis(trimethylsilyl)-1-silacyclopentane-5,5-diyl)[22b] (2.466 and 1.693 Å) and slightly longer than that of *Z*-Tbt(Mes)SiO_2Si(Mes)Tbt[22c] (2.395 and 1.688 Å). The average Si- - -Si distance (2.466 Å) of *dl*-**4** is 9% longer than the Si=Si bond length (2.262 Å) of *dl*-**2**. The average O- - -O distance in the Si_2O_2 ring of *dl*-**4** is 2.333 Å. The torsion angles of Si2−O1−Si3−O2 (0.0°) and Si6−O3−Si6*−O3* (0.2°) indicate that the Si_2O_2 ring is almost planar.

The ^1H NMR spectrum of *dl*-**4** in $CDCl_3$ showed three kinds of peaks assignable to the *tert*-butyl groups. This means that *dl*-**4** has C_2 symmetry through the Si- - -Si axis in the Si_2O_2 ring. The ^{29}Si NMR spectrum of *dl*-**4** in $CDCl_3$ showed two peaks at −54.8 and −2.4 ppm. The former and latter are assignable to the sp^3 silicon atom in the lattice framework and the silicon in the Si_2O_2 ring, respectively.

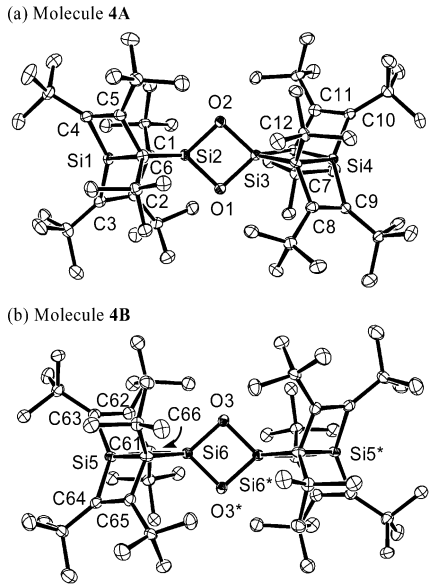

Figure 3. ORTEP drawings of *dl*-**4**. Thermal ellipsoids are drawn at the 50% probability level. Hydrogen atoms are omitted for clarity. Molecules **4A** and **4B** are shown in (a) and (b), respectively.

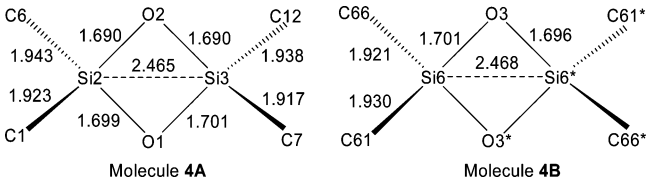

Figure 4. Selected bond lengths (Å) in the Si_2O_2 ring for *dl*-**4**.

Scheme 5

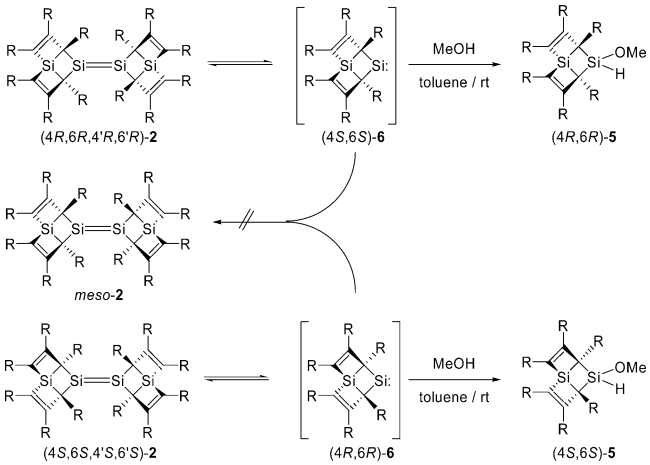

Reaction of *dl*-2 with Methanol. As shown in Scheme 5, the reaction of disilene *dl*-**2** with an excess of methanol in toluene solution at room temperature for 6 days gave **5** in an isolated yield of 94% (Table 2). The structure of **5** was determined by mass spectrometry and ^1H, ^{13}C, and ^{29}Si NMR spectroscopy. Adduct **5**, which is a methanol reaction product of the chiral

(24) (a) Leites, L. A.; Bukalov, S. S.; Garbuzova, I. A.; West, R.; Mangette, J.; Spitzner, H. *J. Organomet. Chem.* **1997**, *536−537*, 425. (b) Leites, L. A.; Bukalov, S. S.; Mangette, J. E.; Schmedake, T. A.; West, R. *Mendeleev Commun.* **1998**, *2*, 43.

Table 2. Reaction of *dl*-2 with Methanol, Acetylenes, and Halides

reagent	irradiation	solvent	reaction time	product (isolated yield)
MeOH	–	toluene	6 days	**5** (94%)
MeOH	–	C_6D_6	12 days	**5** (83%)[a], *dl*-**2** (10%)[a]
MeOH	$h\nu$ (λ > 300 nm)	C_6D_6	20 min	**5** (95%)[a]
bis(trimethylsilyl)acetylene	–	C_6D_6	12 days	**7a** (82%)[a]
bis(trimethylsilyl)acetylene	$h\nu$ (λ > 440 nm)	C_6D_6	3 h	**7a** (90%)[a]
bis(trimethylsilyl)acetylene	$h\nu$ (λ > 440 nm)	hexane	2 h	**7a** (76%)
diphenylacetylene	$h\nu$ (λ > 520 nm)	hexane	25 min	**7b** (quant)
pyridinium tribromide	–	benzene	4 days	**8a** (quant)
CBr_4	–	C_6D_6	2 h	**8a** (53%)[a]
CCl_4	–	C_6D_6	2 h	**8b** (58%)[a]
CCl_4	$h\nu$ (λ > 500 nm)	hexane	14 min	**8b** (quant)

[a] The yield was determined by ^{1}H NMR spectroscopy.

Scheme 6

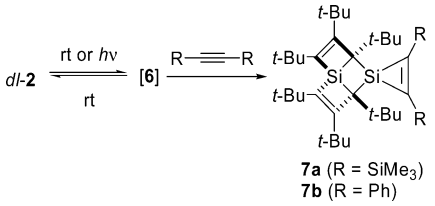

silylene **6**,[25] also was a racemic mixture of (4*R*,6*R*)-**5** and (4*S*,6*S*)-**5**. The formation of **5** confirmed that the thermal equilibrium between *dl*-**2** and **6** exists under such conditions. The equilibrium constant (K = [**6**]^2/[*dl*-**2**]) must be small, because a direct observation of **6** has not been successful using ^{1}H NMR and UV spectroscopy.[26] The *meso*-isomer of **2**, (4*R*,6*R*,4′*S*,6′*S*)-**2**, could possibly be generated by the heterogeneous combination of (4*R*,6*R*)-**6** with (4*S*,6*S*)-**6** in equilibrium. However, *meso*-**2** has not been detected. The experimental result indicates that **6** selectively dimerized into *dl*-**2**.

Interestingly, the following experiment revealed that the dissociation of *dl*-**2** was significantly activated photochemically. A C_6D_6 solution of *dl*-**2** in the presence of methanol was divided into two NMR tubes (samples A and B). Sample A was then immediately used for photolysis, and sample B was stored in the dark as a reference. Photolysis (λ > 300 nm) of sample A for 20 min at room temperature gave **5** in 95% yield, which was determined by ^{1}H NMR spectroscopy. On the other hand, after storing sample B for 12 days at room temperature, **5** (83%) and disilene *dl*-**2** (10%) were observed by ^{1}H NMR spectroscopy.

Reaction of *dl*-2 with Acetylenes. As shown in Scheme 6, the reaction of *dl*-**2** with bis(trimethylsilyl)-acetylene in C_6D_6 at room temperature for 12 days gave **7a** in 82% yield, as determined by ^{1}H NMR spectroscopy (Table 2).[27] The generation of **7a** also indicates the existence of an equilibrium between *dl*-**2** and **6** in solution at room temperature. The irradiation (λ > 440 nm) of *dl*-**2** in the presence of bis(trimethylsilyl)-acetylene in C_6D_6 for 3 h also gave **7a** in 90% yield. The structure of **7a** was established by mass spectrometry and ^{1}H, ^{13}C, and ^{29}Si NMR spectroscopy and was confirmed by X-ray crystallography. Similarly, the irradiation (λ > 520 nm) of *dl*-**2** in the presence of diphenylacetylene in hexane for 25 min gave **7b** quantitatively.[27] The structure of **7b** was established by mass spectrometry and ^{1}H, ^{13}C, and ^{29}Si NMR spectroscopy.

A single crystal of **7a**, suitable for X-ray crystallographic analysis, was obtained by recrytallization from hexane. Crystal data and structure refinement for **7a** are summarized in Table 1. The ORTEP drawing of **7a** is shown in Figure 5. Compound **7a** has C_2 symmetry through the Si1- - -Si2 axis in the solid state. The Si–C and C=C bond lengths in the three-membered ring were 1.835 and 1.357 Å, respectively. The values are similar to the those for 1,1-dimesityl-2,3-bis(trimethylsilyl)-1-silacyclopropene (Si–C: 1.829 Å; C=C: 1.364 Å).[27c]

Reaction of *dl*-2 with Halides. As shown in Scheme 7, the reaction of *dl*-**2** with an excess of pyridinium tribromide gave dibromosilane **8a** quantitatively (Table 2). The structure of **8a** was established by mass spectrometry and ^{1}H, ^{13}C, and ^{29}Si NMR spectroscopy. In the ^{13}C NMR spectrum of **8a** in C_6D_6 at 20 °C, one of the methyl groups in the *tert*-butyl groups was observed around 33.8 ppm as a very broad peak due to the steric hindrance by the introduction of the bromine atoms. On heating to 60 °C, the signal was sharpened and observed at 34.03 ppm. The reaction of *dl*-**2** with tetrabromomethane in C_6D_6 at room temperature for 2 h gave also **8a** in 53% yield as determined by ^{1}H NMR spectroscopy. Similarly, the reaction of *dl*-**2** with tetrachloromethane in C_6D_6 at room temperature for 2 h gave dichlorosilane **8b** in 58% yield, as determined by ^{1}H NMR spectroscopy. Photolysis (λ > 500 nm) of a hexane solution of *dl*-**2** with tetrachloromethane for 10 min gave **8b** quantitatively. Because it is known that the reaction of a dialkylsilylene with chloromethanes gives the corresponding dichlorosilane,[28] the formation of **8a** and **8b** would be explained by the reactions of the intermediate silylene **6** with the halides.

Comparison of the Solid State Structures of *dl*-2, *dl*-4, and 7a. To compare the solid state structures of *dl*-**2**, *dl*-**4**, and **7a**, the selected average bond lengths, bond angles, and torsion angles in the lattice framework of *dl*-**2**, *dl*-**4**, and **7a** are summarized in Table 3. The Si^a–C^a bond length of *dl*-**2** (1.967 Å) is longer than those of *dl*-**4** (1.928 Å) and **7a** (1.903 Å). The C^a–Si^a–C^{a*} bond

(25) The reaction of a cyclic silylene having an asymmetric chiral carbon with alcohols was reported. See: Sanji, T.; Fujiyama, H.; Yoshida, K.; Sakurai, H. *J. Am. Chem. Soc.* **2003**, *125*, 3216.

(26) The preparation of an isolable dialkylsilylene was reported. See: Kira, M.; Ishida, S.; Iwamoto, T.; Kabuto, C. *J. Am. Chem. Soc.* **1999**, *121*, 9722.

(27) Some 2,3-bis(trimethylsilyl)-1-silacyclopropenes and a 2,3-diphenyl-1-silacyclopropene were reported. See: (a) Tsutsui, S.; Sakamoto, K.; Kabuto, C.; Kira, M. *Organometallics* **1998**, *17*, 3819. (b) Ichinohe, M.; Tanaka, T.; Sekiguchi, A. *Chem. Lett.* **2001**, 1074. (c) Ohshita, J.; Honda, N.; Nada, K.; Iida, T.; Mihara, T.; Matsuo, Y.; Kunai, A.: Naka, A.: Ishikawa, M. *Organometallics* **2003**, *22*, 2436.

(28) Ishida, S.; Iwamoto, T. Kabuto, C.; Kira, M. *Chem. Lett.* **2001**, 1102.

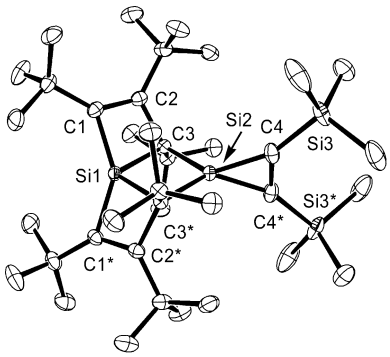

Figure 5. ORTEP view of **7a**. Thermal ellipsoids are drawn at the 50% probability level.

Scheme 7

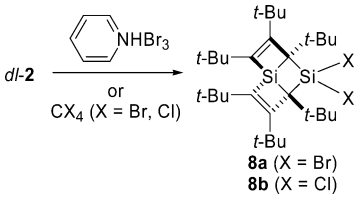

Table 3. Selected Average Bond Lengths (Å), Bond Angles (deg), and Torsion Angles (deg) in the Lattice Framework of *dl*-2, *dl*-4, and 7a

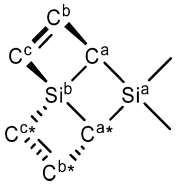

	dl-**2**	*dl*-**4**	**7a**
Si^a-C^a	1.967	1.928	1.903
Si^b-C^a	1.894	1.899	1.915
Si^b-C^c	1.856	1.857	1.850
C^a-C^b	1.577	1.593	1.582
C^b-C^c	1.373	1.373	1.376
$C^a-Si^a-C^{a*}$	89.8	91.1	94.0
$C^a-Si^b-C^{a*}$	94.2	93.0	93.2
$C^c-Si^b-C^{c*}$	147.4	147.1	146.1
$Si^a-C^a-Si^b$	88.0	87.1	86.4
$Si^b-C^a-C^b$	81.9	81.4	81.5
$Si^b-C^c-C^b$	88.9	89.1	89.5
$C^a-C^b-C^c$	107.5	107.7	107.8
$Si^a-C^a-Si^b-C^{a*}$	2.1	2.3	0.0
$C^a-C^b-C^c-Si^b$	14.8	14.2	13.3

angle of *dl*-**2** (89.8°) is narrower than those of *dl*-**4** (91.1°) and **7a** (94.0°). The results are explained by the longer C−Si(sp^2) bond in *dl*-**2** than the C−Si(sp^3) bond in *dl*-**4** and **7a**. The $C^a-C^b-C^c-Si^b$ torsion angles in all the compounds are similar because of the rigidity of the ring.

Theoretical Calculations. In this section, the result of theoretical calculations of *dl*-**2** and the related compounds will be presented. We aim at elucidating the structure of *dl*-**2** and related compounds as well as their energetics using DFT calculations with the Gaussian98 program package.[29,30]

(a) Structure and Energetics of Disilenes. One of the questions about disilene **2** is why only the *dl*-isomer was observed. Formally, the *meso*-isomer of **2** (*meso*-**2**) should also be generated in reaction processes. To answer this question, the structure and energetics of *dl*-**2** and *meso*-**2** were investigated by DFT calculations. Two model disilenes, *dl*-**9** and *meso*-**9**, in which all the *tert*-butyl groups in *dl*-**2** and *meso*-**2** are replaced by hydrogen atoms, were also investigated to evaluate the degree of steric effects caused by bulky substituents. Optimized structures of the disilenes are shown in Figures 6 and 7. Selected geometric parameters and relative energies of the disilenes are listed in Table 4.[31]

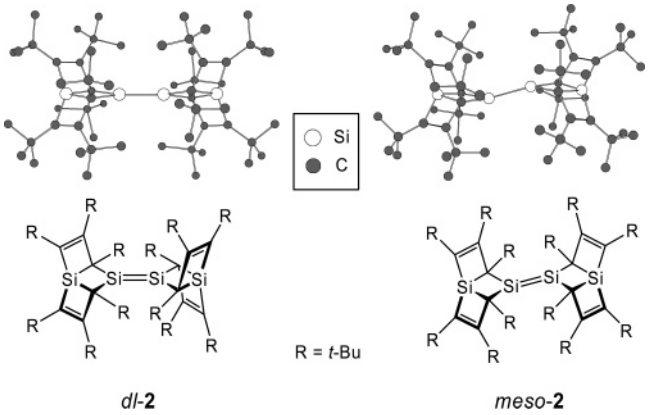

Figure 6. Optimized structures of *dl*- and *meso*-isomers of **2**. Hydrogen atoms are omitted for clarity.

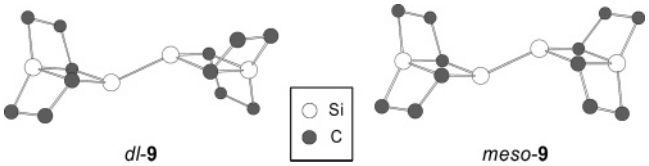

Figure 7. Optimized structures of *dl*- and *meso*-isomers of **9**. Hydrogen atoms are omitted for clarity.

The Si=Si bond distance and the average Si- -Si=Si angle of *dl*-**2** are calculated to be 2.274 Å and 179.1°, while those experimental values based on X-ray structure analysis are 2.262 Å and 177.8°, respectively. Also, the $C^A-Si^B=Si^C-C^D$ torsion angle of *dl*-**2** is as large as 15.5°, which is very close to the measured value (12.1°). The planar and slightly twisted Si=Si bond of *dl*-**2** is nicely reproduced by theoretical calculations. The structure of *meso*-**2** apparently differs from that of *dl*-**2** in the geometry around the Si=Si bond, as shown in Figure 6. The Si=Si bond distance (2.335 Å) of *meso*-**2** is elongated by 0.061 Å relative to that of *dl*-**2**, because of a significant steric repulsion between the *tert*-butyl groups surrounding the Si=Si bond in *meso*-**2**. The

(29) Frisch, M. J.; Trucks, G. W.; Schlegel, H. B.; Scuseria, M. A.; Robb, M. A.; Cheeseman, J. R.; Zakrzewski, V. G.; Montgomery, J. A.; Stratmann, R. E.; Burant, J. C.; Dapprich, S.; Millam, J. M.; Daniels, A. D.; Kudin, K. N.; Strain, M. C.; Farkas, O.; Tomasi, J.; Barone, V.; Cossi, M.; Cammi, R.; Mennucci, B.; Pomelli, C.; Adamo, C.; Clifford, S.; Ochterski, J.; Petersson, G. A.; Ayala, P. Y.; Cui, Q.; Morokuma, K.; Malick, D. K.; Rabuck, D. K.; Raghavachari, K.; Foresman, J. B.; Cioslowski, J.; Ortiz, J. V.; Stefanov, B. B.; Liu, G.; Liashenko, A.; Piskorz, P.; Komaromi, I.; Gomperts, R.; Martin, R. L.; Fox, D. J.; Keith, T.; Al-Laham, M. A.; Peng, C. Y.; Nanayakkara, A.; Gonzalez, C.; Challacombe, M.; Gill, P. M. W.; Johnson, B. G.; Chen, W.; Wong, M. W.; Andress, J. L.; Head-Gordon, M.; Replogle, E. S.; Pople, J. A. *Gaussian 98*; Gaussian, Inc.: Pittsburgh, PA, 1998.

(30) The computational method is based on a DFT calculation with Becke's three-parameter hybrid functional incorporating the Lee−Yang−Parr correlation functional (B3LYP). See: (a) Becke, A. D. *J. Chem. Phys.* **1993**, *98*, 5648. (b) Lee, C.; Yang, W.; Parr, R. *Phys. Rev. B* **1988**, *37*, 785.

(31) Cartesian coordinates of the disilenes studied in this study are presented in the Supporting Information.

Table 4. Selected Geometric Parameters and Relative Stability of Isomers of 2 and 9

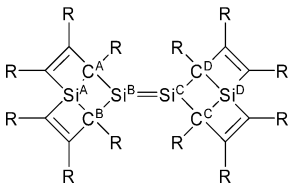

disilene	R	$Si^B{=}Si^C$/ Å	bent angle[a]/ deg	torsion angle[b]/ deg	ΔE/ kJ mol^{-1}
dl-**2**	*t*-Bu	2.274	179.1	15.5	(0)
		(2.262)[c]	(177.8)[c]	(12.1)[c]	
meso-**2**	*t*-Bu	2.335	159.9	0.9	69.8[d]
dl-**9**	H	2.220	143.6	4.5	(0)
meso-**9**	H	2.220	143.6	0.1	0.0[d]

[a] The Si^A- -$Si^B{=}Si^C$ angle. [b]The $C^A{-}Si^B{=}Si^C{-}C^D$ angle. [c]X-ray crystallographic data in ref 16. [d]Energy difference in kJ mol^{-1} relative to the respective *dl*-isomer.

average Si- -Si=Si bond angle (159.9°) of *meso*-**2** indicates that *meso*-**2** adopts a trans-bent Si=Si bond. Neither the trans-bent *dl*-**2** nor the planar *meso*-**2** was found in the present study. Disilene *dl*-**2** is 69.8 kJ mol^{-1} more stable in energy than *meso*-**2**. This result also indicates a larger degree of steric repulsion in *meso*-**2** than that in *dl*-**2**.

The influence of the lattice-framework skeleton of **2** on the structure and stability can be discussed on the basis of a comparison between *dl*-**9** and *meso*-**9**, in which the steric repulsion can be neglected. As shown in Figure 7 and Table 4, the geometric parameters around the Si=Si bond are nearly similar for both *dl*-**9** and *meso*-**9**. The Si- -Si=Si bond angles for both the isomers are as small as 143.6°, which is close to the bent angle (152.6°) of the Si=Si bond in tetramethyldisilene calculated at the B3LYP/6-311+G(d,p) level. This result indicates that the stable structures of *dl*-**9** and *meso*-**9** have a trans-bent Si=Si bond, unlike the structure of *dl*-**2**. The *dl*- and *meso*-isomers of **9** with the planar Si=Si bond were calculated to be transition state structures lying 11.8 kJ mol^{-1} above the corresponding trans-bent isomers. Namely, the planarity of the Si=Si bond in *dl*-**2** stems not from the lattice framework but from the steric repulsion between the *tert*-butyl groups. For the relative stability of *dl*-**9** and *meso*-**9**, both isomers are energetically identical. The results of calculations for the model disilene suggest that the molecular skeleton consisting of four-membered rings has little influence on the structure and relative stability of the isomers. Also, we can conclude that including the bulky *tert*-butyl groups into the calculations is essential for reproducing the experimental results.

The dissociation energy of *dl*-**2** for splitting into two molecules of the corresponding silylene **6** is as small as 48.6 kJ mol^{-1}. This dissociation limit is smaller than the energy gap (69.8 kJ/mol) between *dl*-**2** and *meso*-**2**.[34] On the other hand, the dissociation energy of *dl*-**9** (and *meso*-**9**) is as large as 188.5 kJ mol^{-1}, which is comparable to that of tetramethyldisilene (209.4 kJ mol^{-1}). These results suggest that the steric repulsion between the *tert*-butyl groups reduces the degree of stabilization by forming the Si=Si bond in *dl*-**2**. The small dissociation energy of *dl*-**2** corroborates the presence of a thermal equilibrium between *dl*-**2** and **6** in solution at room temperature.

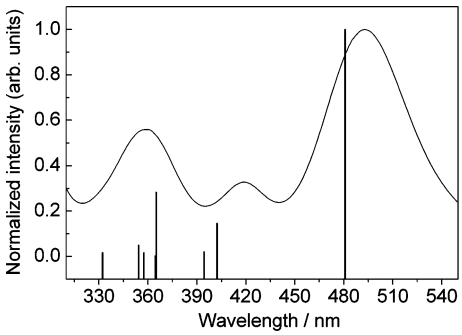

Figure 8. Electron transition energies of *dl*-**2** calculated by the TD-B3LYP method (vertical line). The UV/vis spectrum of *dl*-**2**, in which the intensities are normalized, is also shown for comparison. The calculated intensities are presented using normalized oscillator strengths.

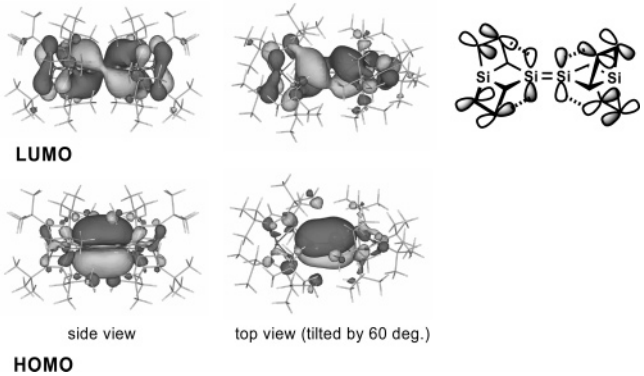

Figure 9. Spatial distribution of the HOMO and LUMO of *dl*-**2**. A schematic diagram of the LUMO is also presented to clarify the $\pi^*{-}\pi^*$ interaction.

(b) Spectroscopic and Magnetic Properties of 2. Disilene *dl*-**2** has the $\pi{-}\pi^*$ absorption maximum at 493 nm, which is significantly red-shifted relative to other tetraalkyldisilenes such as tetramethyldisilene (344 nm).[20] The red-shifted $\pi{-}\pi^*$ absorption of *dl*-**2** is ascribed to the unique electronic structure of **2**.[18] The HOMO−LUMO ($\pi{-}\pi^*$) transition energy of *dl*-**2** obtained with the time-dependent (TD) DFT[35] method is calculated to be 2.58 eV (481 nm). The TD-DFT calculation nicely reproduced not only the positions of the absorption bands but also the relative intensity of the bands in the measured UV−vis absorption spectrum (Figure 8). The red-shifted $\pi{-}\pi^*$ absorption of *dl*-**2** can be associated with a lowering of the LUMO energy level. An intramolecular through-space interaction exists between the $\pi^*_{Si=Si}$ and $\pi^*_{C=C}$ orbitals in the LUMO of *dl*-**2**, contributing to the stabilization of the LUMO, as shown in Figure 9.

(32) Review: Apeloig, Y. In *The Chemistry of Organic Silicon Compounds*; Patai, S., Rappoport, Z., Eds.; Wiley: Chichester, 1989; Chapter 2, p 129.

(33) Karsten, K.-J. *J. Am. Chem. Soc.* **1985**, *107*, 537.

(34) The relative stability and dissociation energy of **2** strongly depend on the quality of the basis sets. For example, at the same level as the optimization was employed, *dl*-**2** is calculated to be 54.5 kJ/mol more stable than *meso*-**2** and the dissociation energy of **6** is calculated to be 94.0 kJ/mol.[17]

(35) (a) Stratmann, R. E.; Scuseria, G. E.; Frisch, M. J. *J. Chem. Phys.* **1998**, *109*, 8218. (b) Bauernschmitt, R.; Ahlrichs, R. *Chem. Phys. Lett.* **1996**, *256*, 454. (c) Casida, M. E.; Jamorski, C.; Casida, K. C.; Salahub, K. D. R. *J. Chem. Phys.* **1998**, *108*, 4439.

Magnetic properties of *dl*-**2** were calculated with the GIAO[36] method at the B3LYP/6-311+G(d,p) level. The ^{29}Si chemical shifts of *dl*-**2** relative to $Si(CH_3)_4$ are calculated to be −6.1 ppm for the sp^3 silicon atoms and 134.7 ppm for the unsaturated silicon atoms. These values reasonably agree with the measured values (−36.7 and 102.5 ppm).

Conclusions

In summary, a one-pot reduction of tri-*tert*-butyl-3-(tribromosilyl)cyclopropene (**1a**) with potassium graphite yielded a unique lattice-framework disilene, a racemate of (4*R*,6*R*,4′*R*,6′*R*)-**2** and (4*S*,6*S*,4′*S*,6′*S*)-**2** (*dl*-**2**). The reactions of *dl*-**2** with methanol, acetylenes, and halides gave the corresponding silylene adducts. Thus, we have succeeded in presenting experimental evidence for the thermal equilibrium between the racemic tetraalkyldisilene *dl*-**2** and the corresponding chiral dialkylsilylene *dl*-**6** in solution at room temperature. Disilene *meso*-**2** has not been observed. Photolysis accelerated the dissociation of *dl*-**2** to **6** in solution. The results of DFT calculations for *dl*-**2** well reproduced the experimental results. The structure and relative stability of the *dl*- and *meso*-isomers of **2** are governed by steric repulsions between the bulky *tert*-butyl groups surrounding the Si=Si bond. The red-shifted $\pi-\pi^*$ transition of *dl*-**2**, which stems from the $\pi^*_{Si=Si}-\pi^*_{C=C}$ bonding interaction in the LUMO, is ascribed to its unique lattice-framework skeleton.

Experimental Section

General Methods. ^{1}H, ^{13}C, and ^{29}Si NMR spectra were recorded on a Varian INOVA 300 FT-NMR spectrometer at 300, 75.4, and 59.6 MHz, respectively. Mass spectra were recorded on Shimadzu GCMS-QP5050A and Hitachi M-2500 mass spectrometers. Electronic absorption spectra were recorded on an Agilent 8453 UV−visible spectrometer. Raman spectra were recorded on a JASCO RMP-200 laser Raman spectrometer. Gel permeation chromatography (GPC) was conducted on an LC908-C60 recycling high-pressure liquid chromatograph (Japan Analytical Instruments Co., Ltd.) with JAIGEL-1H (40 mm × 600 mm), JAIGEL-2H (40 mm × 600 mm), and JAIGEL-2.5H (40 mm × 600 mm) columns using chloroform as the mobile phase and an LC908 recycling high-pressure liquid chromatograph (Japan Analytical Instruments Co., Ltd.) using JAIGEL-1H (20 mm × 600 mm) and JAIGEL-2H (20 mm × 600 mm) columns, using toluene as an eluent.

Materials. Triphenylchlorosilane, magnesium sulfate, aluminum bromide, dry HBr gas, aluminum chloride, dry HCl gas, pyridinium tribromide, and methanol were commercially available and used as supplied. Hexane, toluene, benzene, 3-methylpentane (3-MP), tetrahydrofuran (THF), 2-methyltetrahydrofuran (2-MeTHF), THF-d_6, C_7D_8, and C_6D_6 were freshly distilled over potassium. Tri-*tert*-butylcyclopropenylium tetrafluoroborate[19] was prepared according to the reported procedures.

Preparations. Unless otherwise noted, all operations were performed in oven- or flame-dried glassware under an atmosphere of dry argon.

Preparation of Tri-*tert*-butyl-3-(triphenylsilyl)cyclopropene (3). A THF solution of triphenylsilyllithium [prepared by mixing lithium (1.12 g, 162 mmol) and triphenylchlorosilane (12.0 g, 40.7 mmol) in THF (100 mL)] was added to a mixture of tri-*tert*-butylcyclopropenylium tetrafluoroborate (10.0 g, 33.9 mmol) and THF (100 mL) at 0 °C. After stirring at 0 °C for 2 h, the mixture was hydrolyzed with water. The organic layer was separated, and the aqueous layer was extracted with hexane. The organic layer and the extracts were combined, washed with water and brine, dried over magnesium sulfate, and filtered. The filtrate was concentrated under reduced pressure, and the residue was chromatographed on silica gel using hexane as the eluent. The eluate was concentrated under reduced pressure to leave the crude **3**. Recrystallization from hexane afforded pure **3** (14.2 g, 30.5 mmol, 90%). **3**: colorless crystals; mp 169−170 °C; ^{1}H NMR ($CDCl_3$, δ) 0.94 (s, 9 H), 1.08 (s, 18 H), 7.25−7.33 (m, 9 H), 7.60−7.64 (m, 6 H); ^{13}C NMR ($CDCl_3$, δ) 30.83 (CH_3), 31.51 (C), 31.93 (CH_3), 34.26 (C), 37.70 (C), 124.70 (C), 127.02 (CH), 128.51 (CH), 137.80 (CH), 137.94 (C); ^{29}Si NMR ($CDCl_3$, δ) −14.2; MS (70 eV) *m/z* (%) 409 (M^+ − 57, 34), 207 (100), 78 (96). Anal. Calcd for $C_{33}H_{42}Si$: C, 84.91; H, 9.06. Found: C, 84.94; H, 9.33.

Preparation of Tri-*tert*-butyl-3-(tribromosilyl)cyclopropene (1a). Dry HBr was bubbled through a mixture of **3** (4.91 g, 10.5 mmol), aluminum bromide (0.515 g, 1.93 mmol), and dry toluene (200 mL) for 3 h. After adding acetone (0.3 mL, 4.50 mmol), the resulting mixture was concentrated under reduced pressure, followed by addition of hexane and decantation. The mixture was concentrated under reduced pressure. Bulb-to-bulb distillation [175−220 °C/0.06 mmHg (bath temp)] gave **1a** (4.70 g, 9.89 mmol, 94%). **1a**: colorless crystals; mp 196 °C (dec); ^{1}H NMR ($CDCl_3$, δ) 1.15 (s, 9 H), 1.31 (s, 18 H); ^{13}C NMR ($CDCl_3$, δ) 30.45 (CH_3), 31.11 (CH_3), 31.84 (C), 37.09 (C), 43.70 (C), 123.49 (C); ^{29}Si NMR ($CDCl_3$, δ) −18.1; MS (70 eV) *m/z* (%) 419 (22), 417 (M^+ − 57, 31), 207 (100). Anal. Calcd for $C_{15}H_{27}Br_3Si$: C, 37.91; H, 5.73. Found: C, 37.95; H, 5.79.

Preparation of Tri-*tert*-butyl-3-(trichlorosilyl)cyclopropene (1b). Dry HCl was bubbled through a mixture of **3** (1.05 g, 2.24 mmol), aluminum chloride (0.09 g, 0.67 mmol), and dry benzene (10 mL) for 2 h. The workup similar to that for **1a** gave **1b** (0.46 g, 1.3 mmol, 60%). **1b**: colorless crystals; mp 220−221 °C; bp 80−100 °C/1.0 mmHg (bath temp); ^{1}H NMR ($CDCl_3$, δ) 1.07 (s, 9 H), 1.27 (s, 18 H); ^{13}C NMR ($CDCl_3$, δ) 30.33 (CH_3), 30.71 (CH_3), 31.56 (C), 36.01 (C), 39.91 (C), 122.10 (C); ^{29}Si NMR ($CDCl_3$, δ) 3.9; MS (70 eV) *m/z* (%) 287 (24), 285 (61), 283 (M^+ − 57, 62), 207 (25), 86 (100), 71 (56). Anal. Calcd for $C_{15}H_{27}Cl_3Si$: C, 52.70; H, 7.96; Cl, 31.11. Found: C, 52.76; H, 7.98; Cl, 30.92.

Preparation of Disilene *dl*-2. Dry 2-MeTHF (40 mL) was added to a mixture of **1a** (1.00 g, 2.10 mmol) and KC_8 (0.888 g, 6.57 mmol) at −196 °C. After stirring at −120 °C for 24 h, the mixture was allowed to warm to room temperature. The solvent was then removed in vacuo, and dry hexane was introduced. After the resultant salt and graphite were removed by filtration, the solvent was evaporated in vacuo. Recrystallization from dry hexane gave red-orange crystals of *dl*-**2** (270 mg, 0.290 mmol) in 55% yield. *dl*-**2**: mp 257.5 °C (dec); ^{1}H NMR (C_6D_6, δ) 1.43 (s, 36 H), 1.48 (s, 36 H), 1.64 (s, 36 H); ^{13}C NMR (C_6D_6, δ) 34.39 (CH_3), 34.55 (CH_3), 35.78 (CH_3), 36.06 (C), 36.70 (C), 38.72 (C), 74.34 (C), 164.31 (C), 165.65 (C); ^{29}Si NMR (C_6D_6, δ) −36.7 (SiC_4), 102.5 (Si=Si); MS (14 eV) *m/z* (%) 941 (M^+, 9), 940 (1), 676 (7), 598 (7), 471 (37), 414 (1), 235 (44), 207 (100); UV−vis (hexane) λ_{max}/nm (ϵ) 358 (10000), 419 (5400), 493 (16800); Raman (neat) ν/cm^{-1} (Si=Si) 548. Anal. Calcd for $C_{60}H_{108}Si_4$: C, 76.52; H, 11.56. Found: C, 76.30; H, 11.54.

Oxidation of *dl*-2. A solution of *dl*-**2** (20 mg, 0.021 mmol) in toluene (10 mL) was stirred under an oxygen atmosphere for 1 week. Quantitative oxidation of *dl*-**2** into 1,3,2,4-dioxadisiletane *dl*-**4** was observed by ^{1}H NMR spectroscopy. Recrystallization from toluene gave pure *dl*-**4** (20 mg, 0.021 mmol, quantitatively). *dl*-**4**: colorless crystals; mp 355 °C (dec); ^{1}H NMR (C_6D_6, δ) 1.42 (s, 36 H), 1.50 (s, 36 H), 1.58 (s, 36 H); ^{13}C NMR (C_6D_6, δ) 34.05 (CH_3), 34.25 (CH_3), 35.55 (CH_3), 35.89 (C), 36.41 (C), 38.15 (C), 67.44 (C), 166.81 (C), 168.25 (C); ^{29}Si NMR ($CDCl_3$, δ) −54.8 (SiC_4), −2.4 (Si_2O_2); MS (40 eV) *m/z*

(36) Wolinski, K.; Hilton, J. F.; Pulay, P. *J. Am. Chem. Soc.* **1990**, *112*, 8251.

(%) 973 (M^+, 14), 235 (25), 207 (100). Anal. Calcd for $C_{60}H_{108}O_2Si_4$: C, 74.00; H, 11.18. Found: C, 73.71; H, 11.14.

Reaction of *dl*-2 with Methanol. (a) Dry methanol (25 mg, 7.8×10^{-4} mol) was added to a toluene (15 mL) solution of *dl*-**2** (25 mg, 2.6×10^{-5} mol) at room temperature under argon atmosphere. After stirring for 6 days at room temperature in the dark until the dark red color disappeared, the solvent was removed under reduced pressure. Separation using a recycling GPC (toluene as an eluent) gave the adduct **5** (25 mg, 4.9×10^{-5} mol, 94%). (b) Dry methanol (0.6 mL, 2.4×10^{-5} mol) was added to a C_6D_6 (1.5 mL) solution of *dl*-**2** (0.91 mg, 9.6×10^{-7} mol) at room temperature under an argon atmosphere. The solution was divided into two NMR tubes (samples A and B). Sample A was then immediately used for photolysis, and sample B was stored in the dark as a reference. Photolysis (λ > 300 nm) of sample A for 20 min at room temperature gave **5** in 95% yield, which was determined by ^{1}H NMR spectroscopy. After storing sample B for 12 days at room temperature, **5** (83%) and disilene *dl*-**2** (10%) were observed by ^{1}H NMR spectroscopy. **5**: colorless crystals; mp 186−189 °C; ^{1}H NMR (C_6D_6, δ) 1.34 (s, 9 H), 1.35 (s, 9 H), 1.38 (s, 9 H), 1.39 (s, 9 H), 1.40 (s, 9 H), 1.41 (s, 9 H), 3.49 (s, 3 H), 5.55 (s, 1 H); ^{13}C NMR (C_6D_6, δ) 32.93 (CH_3), 33.53 (CH_3), 33.63 (C), 33.75 (CH_3), 33.81 (CH_3), 34.84 (C), 35.07 (CH_3), 35.20 (CH_3), 35.87 (C), 35.95 (C), 38.14 (C), 38.68 (C), 53.32 (CH_3), 57.25 (C), 59.61 (C), 165.51 (C), 166.22 (C), 166.88 (C, overlapped); ^{29}Si NMR (C_6D_6, δ) −42.0 (SiC_4), −8.6 (SiOMe); MS (70 eV) *m/z* (%) 503 (M^+, 12), 488 (9), 446 (6), 307 (12), 235 (100), 207 (59). Anal. Calcd for $C_{31}H_{58}OSi_2$: C, 74.03; H, 11.62. Found: C, 73.77; H, 11.53.

Reaction of *dl*-2 with Bis(trimethylsilyl)acetylene. (a) A mixture of *dl*-**2** (0.29 mg, 3.1×10^{-7} mol) and bis(trimethylsilyl)acetylene (7.2 μL, 3.2×10^{-5} mol) was dissolved in C_6D_6 (0.8 mL) in a Pyrex NMR tube, and the tube was allowed to stand in the dark at room temperature for 12 days. The ^{1}H NMR spectrum of the reaction mixture showed formation of silacyclopropene **7a** in 82% yield. (b) A hexane (50 mL) solution of *dl*-**2** (21.0 mg, 2.23×10^{-5} mol) and bis(trimethylsilyl)acetylene (528 mg, 3.10 mmol) was irradiated (λ > 440 nm) for 2 h at room temperature under an argon atmosphere. In vacuo evaporation of the solvent resulted in a colorless solid. Recrystallization from hexane gave colorless crystals of silacyclopropene **7a** (13.0 mg, 2.03×10^{-5} mol, 45%). Separation of the mother liquor using a recycling GPC (toluene as an eluent) gave an additional amount of **7a** (8.8 mg, 1.4×10^{-5} mol, 31%). The total yield of **7a** was 76%. (c) A C_6D_6 (0.8 mL) solution of *dl*-**2** (0.35 mg, 3.7×10^{-7} mol) and bis(trimethylsilyl)acetylene (7.2 μL, 3.2×10^{-5} mol) was irradiated (λ > 440 nm) for 3 h at room temperature under an argon atmosphere. The ^{1}H NMR spectrum of the reaction mixture showed the formation of **7a** in 90% yield. **7a**: colorless crystals; mp 241.9−242.3 °C; ^{1}H NMR (C_6D_6, δ) 0.40 (s, 18 H), 1.31 (s, 18 H), 1.35 (s, 18 H), 1.37 (s, 18 H); ^{13}C NMR (C_6D_6, δ) 1.42 ($SiMe_3$), 33.46 (CH_3), 34.11 (CH_3), 34.34 (CH_3), 34.75 (C), 35.61 (C), 38.86 (C), 61.70 (C), 161.34 (C), 167.02 (C), 192.19 (C); ^{29}Si NMR (C_6D_6, δ) −119.0 (SiC_2 ring), −37.6 (SiC_4), −12.1 ($SiMe_3$); UV (hexane) λ_{max}/nm (ϵ) 288 (5790); MS (40 eV) *m/z* (%) 640 (M^+, 3), 568 (8), 470 (35), 207 (100), 155 (77). Anal. Calcd for $C_{38}H_{72}Si_4$: C, 71.17; H, 11.32. Found: C, 70.87; H, 11.18.

Reaction of *dl*-2 with Diphenylacetylene. A hexane (100 mL) solution of *dl*-**2** (19 mg, 2.0×10^{-5} mol) and diphenylacetylene (78 mg, 4.4×10^{-4} mol) was irradiated (λ > 520 nm) for 25 min at room temperature under an argon atmosphere. In vacuo evaporation of the solvent resulted in a colorless solid. Separation of the residue using a recycling GPC (toluene as an eluent) gave **7b** (26 mg, 4.0×10^{-5} mol, quantitatively). **7b**: colorless crystals; mp 206−209 °C; ^{1}H NMR ($CDCl_3$, δ) 1.22 (s, 9 H), 1.27 (s, 9 H), 1.35 (s, 9 H), 7.15−7.38 (m, 10 H); ^{13}C NMR ($CDCl_3$, δ) 32.91 (CH_3), 33.86 (CH_3), 34.05 (CH_3), 34.47 (C), 35.58 (C), 38.56 (C), 62.32 (C), 126.48 (CH), 127.68 (CH), 128.15 (CH), 137.01 (C), 158.70 (C), 162.96 (C), 166.34 (C); ^{29}Si NMR ($CDCl_3$, δ) −96.0 (SiC_2 ring), −39.6 (SiC_4); MS (70 eV) *m/z* (%) 648 (M^+, 6), 591 (3), 470 (2), 207 (100); UV−vis (hexane) λ_{max}/nm (ϵ) 325 (sh, 2200), 275 (sh, 6500), 230 (13000). Anal. Calcd for $C_{44}H_{64}Si_2$: C, 81.41; H, 9.94. Found: C, 81.37; H, 10.03.

Reaction of *dl*-2 with Pyridinium Tribromide. A mixture of *dl*-**2** (50 mg, 5.3×10^{-5} mol), pyridinium tribromide (507 mg, 1.31×10^{-3} mol), and benzene (50 mL) was stirred for 4 days at room temperature. After pyridinium tribromide was removed by filtration, the solvent was evaporated in vacuo. After the resultant solid was dissolved in hexane, the precipitate was removed by filtration. Evaporating of the solvent gave dibromosilane **8a** (66.8 mg, 1.06×10^{-4} mol, quantitatively). **8a**: pale yellow crystals; mp 329−332 °C; ^{1}H NMR (C_6D_6, δ) 1.30 (s, 18 H), 1.44 (s, 18 H), 1.49 (brs, 18 H); ^{13}C NMR (C_6D_6, 20 °C, δ) 33.22 (CH_3), 33.8 (very broad, CH_3), 35.22 (CH_3), 35.42 (C), 36.06 (C), 38.15 (C), 65.63 (C), 166.39 (C), 167.59 (C); ^{13}C NMR (C_6D_6, 60 °C, δ) 33.37 (CH_3), 34.03 (CH_3), 35.38 (CH_3), 35.53 (C), 36.14 (C), 38.19 (C), 66.14 (C), 166.64 (C), 167.84 (C); ^{29}Si NMR (C_6D_6, δ) −38.2 (SiC_4), −7.4 ($SiBr_2$); MS (70 eV) *m/z* (%) 632 (0.5), 630 (0.8), 628 (M^+, 0.5), 573 (0.5), 435 (5), 235 (64), 207 (100). Anal. Calcd for $C_{30}H_{54}Br_2Si_2$: C, 57.13; H, 8.63. Found: C, 57.11; H, 8.53.

Reaction of *dl*-2 with Tetrabromomethane. Tetrabromomethane (16.0 mg, 4.83×10^{-5} mol) was added to a C_6D_6 (7 mL) solution of *dl*-**2** (0.124 mg, 1.3×10^{-7} mol) at room temperature. After allowing the solution to stand at room temperature for 2 h, the ^{1}H NMR spectrum of the reaction mixture showed the formation of dibromosilane **8a** in 53% yield.

Reaction of *dl*-2 with Tetrachloromethane. (a) Tetrachloromethane (692 mg, 5.1×10^{-3} mol) was added to a hexane (50 mL) solution of *dl*-**2** (11 mg, 1.2×10^{-5} mol) at room temperature. After irradiation (λ > 500 nm) for 14 min, evaporation of the solvent gave **8b** (13 mg, 2.4×10^{-5} mol, quantitatively). (b) Tetrachloromethane (19 mg, 1.4×10^{-4} mol) was added to a C_6D_6 (0.7 mL) solution of *dl*-**2** (0.159 mg, 1.7×10^{-7} mol) at room temperature. After allowing the solution to stand at room temperature for 2 h, the ^{1}H NMR spectrum of the reaction mixture showed the formation of **8b** in 58% yield. **8b**: colorless crystals; mp 230−233 °C; ^{1}H NMR (C_6D_6, δ) 1.30 (s, 18 H), 1.40 (s, 18 H), 1.44 (s, 18 H); ^{13}C NMR (C_6D_6, δ) 33.16 (CH_3), 33.4 (very broad, C), 34.92 (C), 35.05 (CH_3), 36.00 (C), 38.17 (C), 64.54 (C), 166.39 (C), 166.93 (C); ^{13}C NMR (C_6D_6, 60 °C, δ) 33.28 (CH_3), 33.64 (CH_3), 35.00 (C), 35.17 (CH_3), 36.07 (C), 38.19 (C), 64.92 (C), 166.59 (C), 167.11 (C); ^{29}Si NMR (C_6D_6, δ) −41.2 (SiC_4), 5.5 ($SiCl_2$); MS (70 eV) *m/z* (%) 542 (44), 540 (M^+, 58), 483 (20), 345 (55), 235 (85), 207 (100). Anal. Calcd for $C_{30}H_{54}Cl_2Si_2$: C, 66.50; H, 10.05. Found: C, 66.80; H, 10.00.

X-ray Crystal Structure Determinations. Intensity data were collected on a Bruker SMART 1000 CCD system[37] using graphite-monochromatized Mo Kα radiation (λ = 0.71073 Å). Using the program SAINT[38] achieved integration. Absorption correction was done by an empirical method using the program SADABS.[39] Subsequent calculations were carried out using SHELXTL.[40] Crystallographic data for the structural analysis have been deposited with the Cambridge Crystallographic Data Center, CCDC Nos. 232428, 232429, and 257922 for *dl*-**2**, *dl*-**4**, and **7a**, respectively. Copies of this information may be obtained free of charge from The Director, CCDC, 12 Union

(37) *SMART* for Windows NT v5.054 Data Collection and *SAINT*+ for NT v5.00 Data Processing Software for the SMART system; Bruker Analytical X-ray Instruments, Inc.: Madison, WI, 1998.

(38) *SAINT* Software Reference Manual, Version 4; Bruker Analytical X-ray Instruments, Inc.: Madison, WI, 1998.

(39) Sheldrick, G. M. *SADABS*; Bruker Analytical X-ray Instruments, Inc.: Madison, WI, 1998.

(40) Sheldrick, G. M. *SHELXTL*; Bruker Analytical X-ray Instruments, Inc.: Madison, WI, 1997.

Road, Cambridge CB2 1EZ, UK (fax: +44-1223-336033; e-mail: deposit@ccdc.cam.ac.uk or www: http://www.ccdc.cam.ac.uk).

Theoretical Calculations. All calculations were carried out using the Gaussian98 program package.[29] The optimized structures of *dl*-**2**, *meso*-**2**, and **6** were computed with the B3LYP hybrid functional.[30] The 3-21G basis sets were employed for the atoms consisting of *tert*-butyl groups, and the 6-31G(d) basis sets were used for the other atoms. Single-point calculations for the energetics of **2** and **6** were carried out at the B3LYP/6-311+G(d,p) level. The model disilene **9** and the corresponding silylene, in which all *tert*-butyl groups in **2** and **6** are replaced by hydrogen atoms, were optimized at the B3LYP/6-311+G(d,p) level. The TD[35] calculations were performed at the B3LYP/6-311+G(d,p) level for the optimized structure described above.

Acknowledgment. We thank Dr. Kenji Yoza of Bruker AXS for fruitful discussions on the X-ray crystallographic analysis.

Supporting Information Available: Tables are available listing the details of the X-ray structure determination, thermal ellipsoid plots, fractional atomic coordinates, anisotropic thermal parameters, bond lengths, and bond angles for *dl*-**2**, *dl*-**4**, and **7a**. Tables are also available listing the Cartesian coordinates of the compounds studied in this study. This material is available free of charge via the Internet at http://pubs.acs.org.

OM050362L